



THE UNIVERSITY *of* EDINBURGH

Edinburgh Research Explorer

Pressure-induced dehydration and the structure of ammonia hemihydrate-II

Citation for published version:

Wilson, CW, Bull, CL, Stinton, G & Loveday, JS 2012, 'Pressure-induced dehydration and the structure of ammonia hemihydrate-II' The Journal of Chemical Physics, vol 136, no. 9, 094506, pp. -. DOI: 10.1063/1.3686870

Digital Object Identifier (DOI):

[10.1063/1.3686870](https://doi.org/10.1063/1.3686870)

Link:

[Link to publication record in Edinburgh Research Explorer](#)

Document Version:

Publisher's PDF, also known as Version of record

Published In:

The Journal of Chemical Physics

General rights

Copyright for the publications made accessible via the Edinburgh Research Explorer is retained by the author(s) and / or other copyright owners and it is a condition of accessing these publications that users recognise and abide by the legal requirements associated with these rights.

Take down policy

The University of Edinburgh has made every reasonable effort to ensure that Edinburgh Research Explorer content complies with UK legislation. If you believe that the public display of this file breaches copyright please contact openaccess@ed.ac.uk providing details, and we will remove access to the work immediately and investigate your claim.



Pressure-induced dehydration and the structure of ammonia hemihydrate-II

C. W. Wilson, C. L. Bull, G. Stinton, and J. S. Loveday

Citation: *J. Chem. Phys.* **136**, 094506 (2012); doi: 10.1063/1.3686870

View online: <http://dx.doi.org/10.1063/1.3686870>

View Table of Contents: <http://jcp.aip.org/resource/1/JCPSA6/v136/i9>

Published by the [American Institute of Physics](#).

Additional information on *J. Chem. Phys.*


Journal Homepage: <http://jcp.aip.org/>

Journal Information: http://jcp.aip.org/about/about_the_journal

Top downloads: http://jcp.aip.org/features/most_downloaded

Information for Authors: <http://jcp.aip.org/authors>

ADVERTISEMENT



AIPAdvances

Special Topic Section:
PHYSICS OF CANCER

Why cancer? Why physics? [View Articles Now](#)

Pressure-induced dehydration and the structure of ammonia hemihydrate-II

C. W. Wilson,^{a)} C. L. Bull, G. Stinton, and J. S. Loveday

SUPA, School of Physics and Astronomy, Centre for Science at Extreme Conditions, University of Edinburgh, Edinburgh EH9 3JZ, United Kingdom

(Received 19 August 2011; accepted 30 January 2012; published online 1 March 2012)

The structure of the crystalline ammonia-bearing phase formed when ammonia monohydrate liquid is compressed to 3.5(1) GPa at ambient temperature has been solved from a combination of synchrotron x-ray single-crystal and neutron powder-diffraction studies. The solution reveals that rather than having the ammonia monohydrate (AMH) composition as had been previously thought, the structure has an ammonia hemihydrate composition. The structure is monoclinic with spacegroup $P2_1/c$ and lattice parameters $a = 3.3584(5)$ Å, $b = 9.215(1)$ Å, $c = 8.933(1)$ Å and $\beta = 94.331(8)^\circ$ at 3.5(1) GPa. The atomic arrangement has a crowned hexagonal arrangement and is a layered structure with long N–D···N hydrogen bonds linking the layers. The existence of pressure-induced dehydration of AMH may have important consequences for the behaviour and differentiation of icy planets and satellites. © 2012 American Institute of Physics. [<http://dx.doi.org/10.1063/1.3686870>]

I. INTRODUCTION

The ammonia hydrates are the simplest systems to incorporate mixed (N–H···O and O–H···N) hydrogen bonds. Such bonds are important biochemically, along with O–H···O H-bonds, mixed H-bonds are responsible for the base-pairings of DNA,¹ and they are responsible for proton transfer reactions in enzymic processes.² Understanding of these bonds and processes rests on knowledge of the relationship between bond strength and geometry,³ and the ammonia hydrates provide a rich range of geometries against which models of such mixed H-bonds can be tested.⁴ The application of pressure provides further insight into the relationships between bond strength and geometry. High pressure allows the geometry of bonds to be continuously and cleanly varied and the changes produced by its application are much larger than those produced by changing temperature. Furthermore, high-pressure structures provide access to arrangements which are not present in ambient pressure phases,⁵ increasing the range of geometries that can be studied. The high-pressure properties of the ammonia hydrates are also directly relevant to modelling of the outer solar system. The outer solar system contains large quantities of ices (water, ammonia, and methane) (Refs. 6 and 7) and these systems and their binary and ternary mixtures form significant fractions of the outer planets Uranus and Neptune and the large icy moons such as Titan, Triton, and the dwarf planet Pluto. Hence, the ammonia hydrates are the most likely ammonia-containing phases in these bodies and their high-pressure properties are crucial input parameters for modelling. For example, convection in the icy mantles of Uranus and Neptune is believed to be origins of their multipolar magnetic fields.⁸ These mantles are believed to be composed of water, ammonia, and methane and the properties and speciation of the materials inside these icy layers are crucial to modeling of these bodies.³⁷

^{a)}Electronic mail: c.wilson-10@sms.ed.ac.uk.

A. The ammonia hydrates

At ambient pressure there are three known stable ammonia hydrates.⁴ Ammonia dihydrate (ADH, $\text{NH}_3 \cdot 2\text{H}_2\text{O}$), has a cubic structure with orientational disorder of the water molecules while the ammonia molecules are ordered. Ammonia monohydrate (AMH, $\text{NH}_3 \cdot \text{H}_2\text{O}$), has an orthorhombic structure with all molecules orientationally ordered. Ammonia hemihydrate (AHH, $2\text{NH}_3 \cdot \text{H}_2\text{O}$), is again orthorhombic but has orientational disorder of one of the two ammonia sites whereas the other ammonia and the water molecules are ordered. AHH was extensively studied from a proton transfer perspective by Bertie *et al.*^{38–40} through infrared spectroscopy. In these studies it was found that AHH, while having a hydrogen bonded network and in that respect similar to water ice, the molecule responsible for proton transfer in AHH was ammonia rather than water.

B. High-pressure studies

The first high-pressure study on solid ammonia hydrates was performed by Nicol and co-workers^{11,12} who concentrated on compositions with a water content of 50% and greater because the water-rich side of the phase diagram is of most relevance to the solar system which is believed to contain ammonia and water in the ratio of 15:85.⁶ The technique they used was visual observation of the sample and crystal morphology in polarised and un-polarised light. Phase identification was then attempted on the basis of comparison with the ambient-pressure forms of AMH and ADH and the known phases of ice. The melting lines of both the ADH and AMH compositions shown in Figures 1 and 2 are derived from the results of these two studies. Boone and Nicol¹² also identified a quadruple point between ADH, ice VIII, ammonia-water fluid and what they assumed was AMH at 245 K and 2.3 GPa. At pressures above this quadruple point, the boundary (subsequently termed a dehydration boundary by Fortes *et al.*¹³) shown as a dotted line in the solid region of the phase

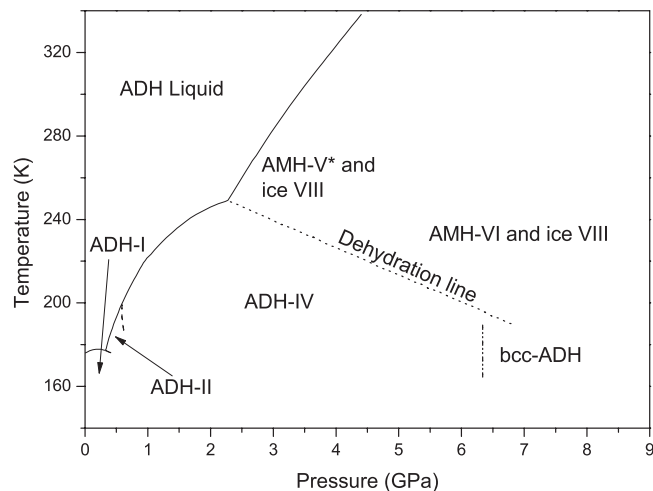


FIG. 1. The phase diagram of ammonia dihydrate after Ref. 9. The diagram has been updated from the source to take into account the fact that Fortes *et al.*¹⁰ showed that ADH-III was a mixture of AMH-II and ice II (see text). (*) The phase shown here to be AMH-V is actually the phase AHH-II (see text).

diagram divides solid ADH from a mixture of what Boone and Nicol proposed was solid AMH and ice.¹² Although no structural studies were performed, Nicol and Johnson¹¹ concluded that in the case of AMH, their visual observation and Raman data showed that the ambient pressure phase persisted up to at least 14.7 GPa. In the case of ADH, Boone and Nicol came to no conclusion about structural transitions, but noted Lunine and Stevenson's argument based on the known density change on melting at ambient pressure and Nicol and Johnson's observed melting line¹¹ that there had to be a structural phase-transition under pressure.⁷ Hogenboom *et al.* subsequently made volumetric measurements along the melting lines of both ADH and AMH in the pressure range of 0–0.4 GPa.¹⁴ From the measured changes in density iden-

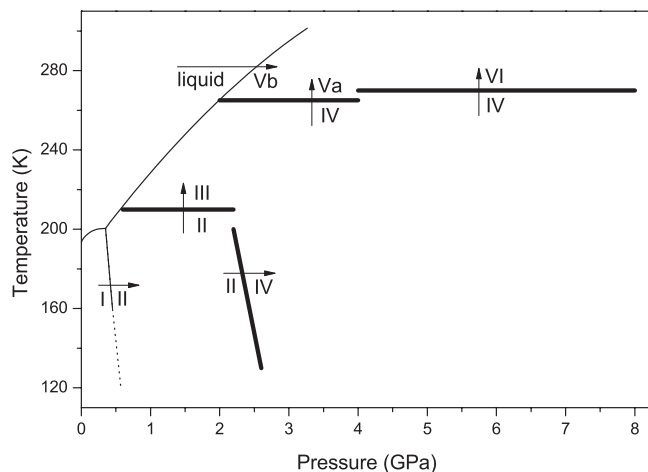


FIG. 2. The phase diagram of ammonia monohydrate after Ref. 15. The melting line is taken from Boone and Nicol¹² and the lines show the P or T conditions under which the transformations are observed when changing the P or T in the direction shown by the arrows. Since, with the exception of I to II and liquid to Va, none of the transitions have been reversed. The thicker lines shown are not thermodynamic phase boundaries but simply provide a guide to the conditions under which transformation occurs.

tified the high-pressure polymorphs ADH-II and AMH-II (Figures 1 and 2). By comparison of the morphologies of *in situ* grown single crystals, Fortes *et al.*¹⁰ were able to show that the ADH phase studied by Boone and Nicol¹² was in fact ADH-IV (see below).

1. Ammonia monohydrate at pressure

The first diffraction based study of the phase diagram of AMH was carried out by Loveday and Nelmes using neutron diffraction.¹⁵ They found six high-pressure forms, phases II, III, IV, Va, Vb, and VI (see Figure 2). The nomenclature for phase V was chosen because phases Va and Vb are produced by different paths and have similar diffraction patterns suggesting that their structures may be related. Of all these high-pressure phases, only the structure of phase VI was solved¹⁶ and shown to be a substitutionally disordered molecular alloy whose structure is related to that of ice VII, this structure was subsequently also found in ADH (see below). Compression at 130 K suppresses the AMH-I to II transition and allowed a determination of the equation of state of AMH-I with $B_0 = 8.9(4)$ GPa and $B' = 4.2(3)$ over the range 0–3 GPa.¹⁵ Fortes *et al.* also solved the structure of AMH-II based on *ab initio* density functional theory predictions of the structure which were confirmed and refined using neutron-diffraction data.^{17–19} These showed it to be orthorhombic with an ordered proton arrangement.

2. Ammonia dihydrate at pressure

The behaviour of ADH has been extensively explored by Fortes *et al.*^{10,13,20,21} They measured the compressibility of ADH-I using neutron diffraction²⁰ and obtained a value of $B_0 = 7.0(2)$ GPa and $B' = 9(1)$ which compared reasonably with that calculated from density functional theory.²¹ In subsequent work, Fortes *et al.*¹³ observed three more ADH phases, phases III, IV and, transiently in a single sample, a body centred cubic structure which appeared to be the ADH composition variant of the AMH-VI structure which has substitutional site disorder of the ammonia and water molecules (see above). They also confirmed the dehydration line reported by Boone and Nicol. At pressures and temperatures above this line, they observed mixtures of ice VII or VIII (depending on the temperature) and either AMH-V (Fortes *et al.* did not distinguish between AMH-Va and Vb) or AMH-VI. Fortes *et al.*¹³ commented that the behaviour in the low pressure region was complex and were unable to obtain reproducible relative intensities. Subsequent further studies showed that ADH-II consists of two phases with very similar densities whose relative proportions depend on the path taken and the rate of temperature and/or pressure change.¹⁰ Fortes *et al.* were also able to show that ADH-III was in fact a mixture of ice II and AMH-II.¹⁰ Although the transition between ADH-II and ADH-IV has never been observed, ADH-IV was found to form consistently from the melt between 0.6 and 2.4 GPa^{10,13} and has a orthorhombic unit cell.¹⁰ Loveday *et al.*⁹ showed that ADH-I amorphises if compressed at 170 K. (Amorphisation is attributable to the use of a Paris-Edinburgh press rather

than a gas cell, both Nelmes *et al.* and Fortes *et al.* observe the phase I to II transition when a gas cell is used.^{20,22}) This amorphous ADH when compressed to 4 GPa and above at 170 K and warmed transformed to the bcc AMH-VI structure with the ADH composition at ~ 270 K. Furthermore, it was shown that this substitutionally disordered form could be made reproducibly and remained stable at room temperature.⁹

3. Ammonia hemihydrate at pressure

To date no high-pressure studies of AHH have been published and hence nothing is known about its high-pressure phase diagram. This may be because there is no evidence for the dehydration of AMH at any pressure or temperature combined with the fact that the outer solar system is believed to be water rich. Thus, based on evidence to date, it is unlikely that AHH is found anywhere in nature and so its high-pressure behaviour has not been explored.

C. Concluding introductory remarks

Out of all the ammonia-hydrate phases known, that currently referred to as AMH-V stands out as important. Because of the ADH dehydration line (see above), it is likely to be the ammonia-bearing phase formed at ambient temperature and above by the ammonia-water mixtures found in the solar system and it is stable up to at least 14.7 GPa.^{11,15} As such it occupies a significant part of the phase diagram and is a major potential-component of icy planets and moons. Its wide range of stability also means that it also provides a good system to follow the pressure dependence of the bond geometries. In this paper, we present combined synchrotron x-ray single-crystal and neutron-powder diffraction studies of the solid phase formed when a 1:1 ammonia hydrate liquid is compressed at room temperature—the phase called AMH-Vb by Loveday and Nelmes.¹⁵ These have revealed the surprising result that it is not a single phase of ammonia monohydrate as had been previously thought but a mixture of an ammonia hemihydrate solid and ice VII. We have now been able to solve the structure of the ammonia hemihydrate (ammonia hemihydrate-II) and so show that it has a molecular packing similar to that of ice VII.

II. EXPERIMENTAL

Samples were prepared for both x-ray single-crystal and neutron-powder experiments by similar procedures. Ammonia gas (99.99% purity) obtained from Sigma-Aldrich and distilled water (99.9% purity) were used to create the 1:1 molar ratio of ammonia to water (for the neutron-diffraction studies deuterated water (99.98% deuterated) and ammonia (99% deuterated), again from Sigma-Aldrich, were used²³). Ammonia was condensed at liquid-nitrogen temperature into a preweighed stainless-steel bottle. The bottle was sealed, warmed and the amount of ammonia condensed measured by weighing the bottle again. The correct mass of water to create a 1:1 molar mixture was put into a second steel bottle which was again sealed and the two bottles were connected together

by a steel tube. The bottle containing the water was cooled in liquid nitrogen while the other, containing the ammonia, was held at room temperature. The valves sealing the bottles were opened and the ammonia condensed into the cold bottle containing the water(ice). The valves were then closed and the bottle containing the ammonia/water mixture was allowed to warm and shaken to ensure full mixing. The final composition was checked by further weighing of the bottle and the mixed solution and was found to have a composition within 3.0(1)% of the target 1:1 ratio.

To load the sample for the x-ray experiment, it was first stabilised as a liquid by cooling the bottle with a freezing mixture made from isopropyl alcohol (IPA) and liquid nitrogen, which provides a stable temperature of 185 K. Drops of the liquid sample were allowed to fall onto the 80 μm thick preindented T301 steel gasket, with a 150 μm hole, mounted in a Merrill-Bassett diamond anvil cell (DAC)²⁴ with 400 μm diamond culets, which had been precooled to 77 K. The cell was closed, sealed, and allowed to warm to room temperature. The sample was compressed until it become solid at a pressure, measured by ruby fluorescence, of 3.6(4) GPa.

The loaded sample, when viewed optically, consisted of many very small crystallites. The sample was transparent to visible light and also allowed light to pass through when placed between two crossed polarisers. Optically isotropic materials, such as liquids and unstrained cubic crystals, will not allow light to pass through crossed polarisers as they do not change the polarisation of the light. It thus appears that unlike ice VII, the cubic phase of ice which is stable at these pressures and temperatures, the ammonia hydrates formed at these pressures and temperatures are optical anisotropic and can be distinguished from ice and molten sample by their birefringence.

A single-crystal was grown *in situ* by heating the sample and melting the crystallites until only one remained, which was allowed to grow to fill the sample volume as the cell was slowly cooled back to room temperature. However, the single crystal that was grown failed to fill the entire sample volume, suggesting that either the composition of the sample as loaded was not the 1:1 originally made – it is possible that some ammonia had been lost during cell loading – or that the crystal formed did not have a 1:1 ammonia water ratio.

Single-crystal x-ray data were collected at the ID09a beam line at the European Synchrotron Radiation Facility (ESRF) in Grenoble, France. The detector used was a Mar555 detector. The beamline was calibrated with a silicon standard sample which determined the wavelength to be 0.4142(2) Å. The data were collected with an exposure time of 1 s per step angle of 0.25° over a $\pm 30^\circ$ range either side of the cell's axis.

For the neutron-diffraction experiments, the deuterated 1:1 sample was loaded by first stabilising the sample by cooling with a CO₂ and IPA freezing mixture and the cooled liquid was dropped into one of the two tungsten-carbide anvils of a Paris-Edinburgh press²⁵ precooled to liquid-nitrogen temperature as described by Loveday *et al.*¹⁶ Once assembled, the anvils were loaded into the press and a sealing-load of 5 tonnes was applied to them. The press was then left to warm to room temperature and dry. Neutron-diffraction data were collected on the PEARL instrument of the ISIS pulsed

neutron source at Rutherford Appleton Laboratory, UK. PEARL has the capability to operate at temperatures down to 77 K and to check the composition of the sample, the press was then cooled to 150 K and a neutron time-of-flight diffraction pattern was collected at the low sealing load (5 tonnes). The pattern observed was that of the known ambient-pressure structure of ammonia monohydrate⁴ with no evidence of either excess ice or of any other ammonia hydrate in the pattern. This confirms that the composition of the mixture loaded was the 1:1 ratio intended. The press was warmed back to room temperature and neutron-diffraction patterns were collected as a function of increasing applied load. Once crystallisation had occurred, data were collected with the pressure cell in two orientations. In the transverse orientation, the incident beam entered the cell along its axis and the diffraction signal was recorded by detectors centred at $2\theta = 90^\circ$ which access d-spacings in the range 0.5–4.2 Å. Data collection times for this arrangement were between three and six hours. In the longitudinal orientation, the incident beam enters through the gasket and diffraction is observed by detectors centred at $2\theta = 30^\circ$ which provide access to d-spacings in the range 1–12 Å. The smaller solid angle of these low-angle detector meant that data collection times for this orientation were longer (between eight and twelve hours). The data were corrected for variation in the incident neutron spectrum and for the effects of attenuation by the pressure cell using the procedures described by Wilson *et al.*²⁶

III. STRUCTURE ANALYSIS

From analysis of the x-ray diffraction pattern, a unit cell was determined with lattice parameters of $a = 3.396(1)$ Å, $b = 9.254(1)$ Å, $c = 9.006(2)$ Å, $\alpha = 90.05(1)^\circ$, $\beta = 94.40(1)^\circ$, and $\gamma = 90.06(1)^\circ$ at 3.6(4) GPa. The unit-cell symmetry was examined using the XPREP software²⁷ and the systematic absences and equivalencies of reflections were consistent with the spacegroup of $P2_1/c$. Although this space group has unique absences, at this stage it could not be ruled-out that the full structure (with hydrogen atoms) had the symmetry of one of two subgroups $P2_1$ and Pc .

The unit cell derived from the x-ray data, was then used as a starting point to examine the neutron data. The upper plot of Figure 3 shows a Le Bail fit to the neutron data using only the unit cell and symmetry derived from the x-ray data along with the scattering expected from the pressure-cell materials close to the sample. There is good correspondence between the peak positions expected for the monoclinic cell but there are some significant unfitted, and hence unindexed, peaks, most notably that at 2.35 Å as shown in the inset. The position of this peak corresponds well with that expected for the strongest (110) peak of ice VII (the stable phase of ice at this pressure).²⁸ Inclusion of ice VII as an additional phase in the refinement produced a fit (Figure 3, lower) which accounts for all peaks observed. The presence of ice VII in this high-pressure pattern was a surprise. However, given that the sample had been shown to have the AMH composition by diffraction studies close to ambient pressure (see above) the existence of free ice in the high-pressure data suggests that the ammonia-bearing monoclinic high-pressure hydrate

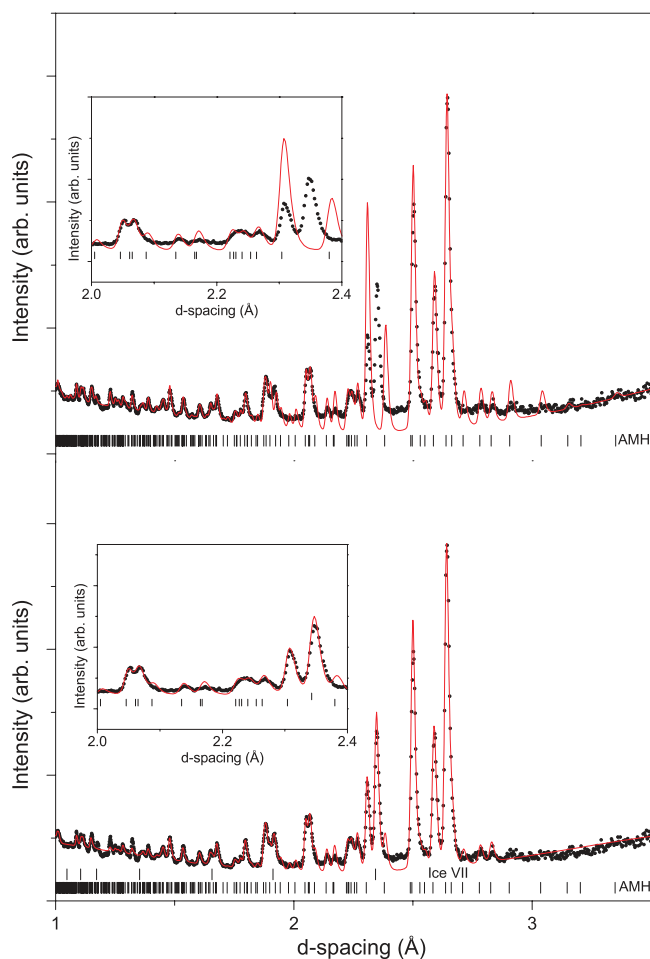


FIG. 3. Le Bail fits of the neutron-diffraction data, the dots show the observed data points and the lines show the calculated fits to the data. The upper plot fits using only the monoclinic unit cell of the ammonia hydrate determined from x-ray single-crystal data and the lower fits using this cell and that of ice VII. The vertical lines denote the expected positions of reflections which are labelled to show which phase they represent. The inset shows a close up of the d-spacings around the ice peak.

is significantly richer in ammonia than the 1:1 AMH composition loaded.

This result is somewhat surprising given that Boone and Nicol¹² concluded that at this pressure and temperature they observed AMH and, depending on the composition of their sample, ice. However, it should be noted that they only studied a single 1:1 composition sample and that the sample was powdered which may have hampered identification of the ice. From their extensive exploration of the ADH/AMH stability regions in solutions with a 1:2 ammonia water ratio, it would have been difficult to estimate the amount of ice produced when the sample decomposed into ice and an ammonia-hydrate and hence the amount of water contained in that ammonia hydrate. For these reasons we would argue that our diffraction results do not contradict those of Nicol and co-workers, but simply are the result of our better sensitivity.

As previously stated, the composition of the new ammonia hydrate is richer in ammonia than 1:1. Unfortunately, the only composition for which equation of state data are known is AMH.²⁹ However, the average volume per molecule (taken

over both water and ammonia) for ADH, AMH, and AHH at ambient pressure are, respectively, $30.170(6) \text{ \AA}^3$, $30.604(2) \text{ \AA}^3$ and $30.583(2) \text{ \AA}^3$.⁴ These values are very similar and show no obvious trend between volume per molecule and composition. It thus seems reasonable to assume that the ammonia hydrates also show no significant composition dependence in their equations of state. The contents of the unit cell can thus be estimated from the equation of state of AMH-I (Ref. 29) based on the assumption that the mean volume per molecule at pressure is not significantly different from that of AMH. The equation of state of AMH gives a mean volume per molecule of $\sim 23.8 \text{ \AA}^3$ at $3.6(4) \text{ GPa}$ which would suggest that the monoclinic cell of volume $282.2(1) \text{ \AA}^3$ contains 12 molecules. However, given the uncertainty of the composition it is not possible to be certain how many of these molecules are ammonia and how many are water (except that the ammonia:water ratio must be greater than the 1:1 of the starting material).

The quality of the x-ray data was not sufficient to yield a plausible solution from direct methods and so the FOX software package was used to try and find a starting molecular arrangement from the x-ray data using simulated annealing.^{30,31} The spacegroup $P2_1/c$ allows two ways to accommodate twelve molecules. The molecules could either be distributed over three general (four-fold sites) or two general and two special (two-fold) sites and all possibilities were tested against the data. Because ammonia and water are isoelectronic and the exact composition of the hydrate was not known, all molecular sites were made to have the same scattering factor. After several runs of the parallel tempering algorithm, the three general sites structure repeatedly gave similar structures as the best fitting with a goodness of fit (G-o-F) of 3685. In comparison, the two general and two special position models gave a G-o-F of 9760.³²

The neutron data were then further checked for evidence that the spacegroup was indeed $P2_1/c$. No evidence was found of any reflections violating this symmetry in either the longitudinal or transverse diffraction patterns. And specifically no evidence was found in the longitudinal data for the long d-spacing reflections predicted for spacegroups Pc and $P2_1$. It thus appears that the space group is indeed $P2_1/c$.

The arrangement derived from FOX was then tested against the neutron-powder data to determine the full structure using the GSAS refinement package.³³ Because the precise composition was unknown, the starting model used had substitutional disorder of oxygen and nitrogen on the molecular centres given by FOX and orientational disorder of the molecules to produce four deuterium sites arranged in a tetrahedron around the molecular centres at a distance of 1 \AA from them. The occupancies of these sites were adjusted to give the correct total number of atoms, so that a molecular site which was half occupied by water and half by ammonia had four deuterium-sites each containing 0.625 of an atom giving a total of 2.5 deuterium atoms per molecule.

The above model was refined against the neutron data. In the refinements the occupancy of the molecular-centre sites and orientations of the tetrahedra were allowed to vary. These procedures sought to determine whether the molecule on a

particular site was a water molecule, an ammonia molecule, or a disordered site containing both types of molecule. The refinement was subject to constraints so that the total occupancy of the molecular site was held to one, that the deuterium occupancy was consistent with the N/O occupancy (three deuterium atoms per nitrogen and two per oxygen), and that the geometry of the tetrahedra remained fixed. Refinement of the occupancies and orientation improved the fit from a R_{wp} of 7.405% to 6.487% and converged with one site oxygen-rich and the other two sites nitrogen-rich suggesting a composition close to or at ammonia hemihydrate. The other two possible configurations of two ammonia molecules and one water spread over three centres gave poorer fits ($R_{wp}=8.447\%$ and 8.367%). The occupancy of the D sites was then adjusted to the ideal values of the new configuration, so that around the N atoms the four sites had a starting occupancy of 0.75 and around the oxygen centre the occupancies were 0.5. The occupancy of all the deuterium atoms associated with one molecular centre site were then allowed to refine freely, this was then repeated for the other molecular centre sites separately. The deuterium site that was the least occupied was set to zero and the remaining were refined again so that in the end each nitrogen site was surrounded by three approximately fully occupied D site and each oxygen by two approximately fully occupied D sites. This suggests strongly that not only is the basic structure a hemihydrate, but it also has fully ordered molecular orientations. For the final refinement shown in Figure 4, the occupancies of all occupied sites were fixed to one and the rigid body constraint was removed to allow the internal molecular geometry to vary. The final refinement shown gave a weighted profile R factor (R_{wp}) of 3.3% with 76 fitting parameters.³⁴ The unit cell from the refinement of the neutron data was slightly different from that of the x-ray data, with the parameters being $a = 3.3584(5) \text{ \AA}$, $b = 9.215(1) \text{ \AA}$, $c = 8.933(1) \text{ \AA}$, and $\beta = 94.331(8)^\circ$. The pressure of the neutron sample can be calculated from the equation of state of

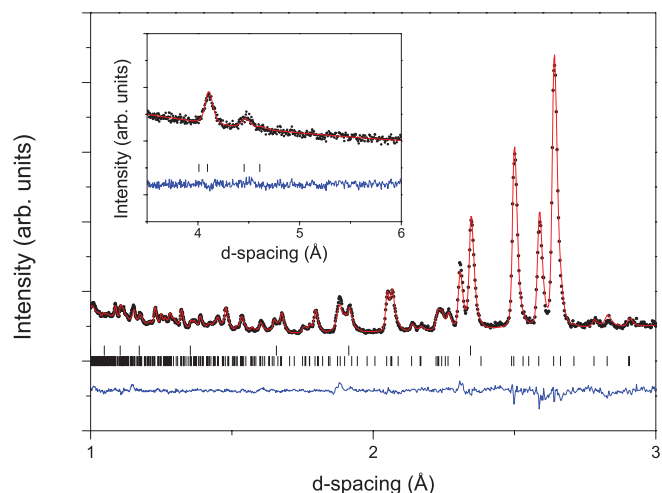


FIG. 4. Rietveld profile refinement of AHH structure and ice VII to the neutron powder data. The dots show the observed data points, the line close to the data points show the calculated fits, the lower line the difference between observed and calculated plots, and the vertical lines show the expected positions of reflections as per Figure 3. The inset shows the high d-spacing data obtained in the longitudinal orientation (see text).

the ice VII in the sample volume²⁸ and was found to be 3.5(1) GPa.

The quality of fit shown in Figure 4 is excellent and the bond lengths and angles are all plausible and within expected ranges (see Table II). Furthermore, the refined ratio of ice VII to ammonia hydrate is 1:2.30(5) in the pattern shown in Figure 4. While the discrepancy between the ideal case and what was produced by refinement may at first seem rather large, the phase fraction ratio of 1:2.3, which is based on the ratio of the number of unit-cells, corresponds to an ammonia:water ratio of 1:1.075. However, data were collected from two other samples with a 1:1 composition. These samples produced the same high-quality fits with the same AHH structure but scale factor ratios of 1:4.7(1) and 1:4.9(1), respectively. This raises the possibility that the structure is richer in ammonia than AHH and that there is partial substitution of ammonia onto the water site. Refinements using such a model produced evidence for an occupancy of $\sim 10\%$ of ammonia on the water site with a small improvement (R_{wp} of 3.2%) in the quality of fit which suggests a 95% level of confidence.⁴¹ Given the uncertainties in performing significance tests on powder data it will require single-crystal neutron data to confirm this partial ammonia occupancy of the water site, but the amount involved cannot in any case explain the scale factor ratios. Instead it seems that the anomalous scale factor ratios arise from samples that are spatially inhomogeneous combined with the fact that some 20–30% of the sample volume is not illuminated by the beam. Further more, the diffraction signal from the ice VII was observed to be textured, which also affects the relative intensities of the ice VII and hence the phase fraction. While it is unsatisfactory that the phase fraction cannot be reconciled it should be noted that all three samples give high-quality fits with the same AHH structure in spite of the strong variation in the amount of ice VII observed.

For these reasons and the fact that the refined structural co-ordinates given in Table I and the bond lengths and angles given in Table II are extremely reasonable we argue that the structure is correct and that the phase labelled AMH-Vb by Loveday and Nelmes¹⁵ is in fact a structure of ammonia hemihydrate and should be called AHH-II.

TABLE I. Coordinates of AHH structure at 3.5(1) GPa obtained from neutron data, all atomic sites are on 4e (x,y,z) Wyckoff positions.

| Atom | x | y | z | $U_{iso} \times 10^2 (\text{\AA}^2)$ |
|------|----------|----------|----------|--------------------------------------|
| N1 | 0.714(2) | 0.129(1) | 0.413(1) | 0.56(8) |
| D1 | 0.821(3) | 0.043(1) | 0.370(1) | 1.2(1) |
| D2 | 0.792(2) | 0.133(1) | 0.528(1) | 1.2(1) |
| D3 | 0.406(3) | 0.146(1) | 0.401(1) | 1.2(1) |
| O1 | 0.039(3) | 0.867(2) | 0.238(1) | 0.56(8) |
| D4 | 0.135(4) | 0.783(1) | 0.185(1) | 1.2(1) |
| D5 | 0.150(3) | 0.956(1) | 0.196(1) | 1.2(1) |
| N2 | 0.665(2) | 0.875(1) | 0.898(1) | 0.56(8) |
| D6 | 0.751(3) | 0.876(2) | 0.008(1) | 1.2(1) |
| D7 | 0.715(3) | 0.772(1) | 0.855(1) | 1.2(1) |
| D8 | 0.380(3) | 0.896(1) | 0.890(1) | 1.2(1) |

TABLE II. The X...Y and X-D distances of all hydrogen bonds (X-D...Y) in the structure of AHH-II.

| Atoms | H-bond length(\AA) | Atoms | Covalent bond length(\AA) |
|---------|--------------------|-------|---------------------------|
| N1...O1 | 3.162(11) | N1-D1 | 0.967(14) |
| N1...O1 | 3.116(15) | N1-D2 | 1.042(8) |
| N1...N1 | 3.3585(5) | N1-D3 | 1.042(11) |
| O1...N1 | 2.739(16) | O1-D4 | 0.974(17) |
| O1...N2 | 2.880(20) | O1-D5 | 0.983(20) |
| N2...O1 | 3.314(15) | N2-D6 | 1.012(9) |
| N2...O1 | 3.204(12) | N2-D7 | 1.044(14) |
| N2...N2 | 3.3585(5) | N2-D8 | 0.976(10) |

IV. CRYSTAL STRUCTURE

Figure 5 shows the structure as viewed down the *a* axis, this can be described in full by a series of chair configuration hexagonal rings each “crowned” by an ammonia molecule that has one bond that points near parallel to the *a* axis. Hexagon A is marked out by the ring of molecules N1a, O1b, N2c, O1c, N1c, O1a and crowned by the molecule N2b. If only the molecular centres of these molecules were to be considered, then this unit would tile the entire *b-c* plane of the structure with very minor positional differences. However, the orientation of the hydrogen bonds complicate this somewhat and require another three crowned hexagons to be defined to reproduce the structure in full. These are marked in the figure as Hexagon A' (formed by N2a, O1a, N1c, O1d, N2c, O1b and crowned by N1b), A'' (formed by N1c, O1c, N1a, O1a, N2a, O1d and crowned by N2b) and A''' (formed by N2c, O1d, N2a, O1b, N1a, O1c and crowned by N1d). These are all hexagons crowned by ammonia molecules that have a bond nearly parallel to the *a* axis. Alternately a set of four hexagons that are crowned by ammonia molecules with a hydrogen bond that have a bond near anti-parallel with the

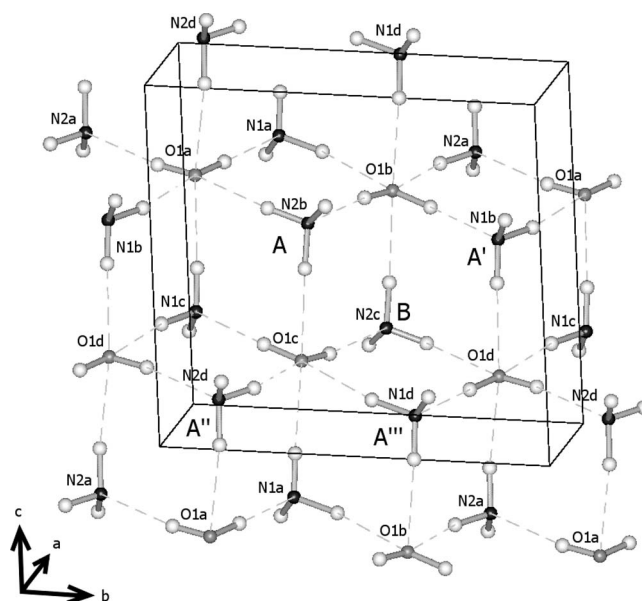


FIG. 5. The structure of AHH-II viewed approximately along the *a* axis. The black balls represent nitrogen atoms, the grey oxygen atoms, and the white hydrogen atoms. The hydrogen bonds are shown as dashed lines.

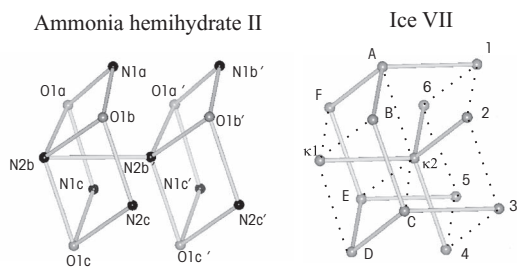


FIG. 6. Left: The crowned hexagon A of AHH-II as described in the text showing the stacking of adjacent hexagons along the a -axis. The solid lines show H-bonds, for clarity the hydrogen atoms have been omitted. Right: The analogous capped ring structure in ice VII. The solid lines represent H-bonds and the dotted lines represent non-bond $O \cdots O$ contacts whose length is identical to that of the H-bonds. Again for clarity the hydrogen atoms have been omitted.

a axis can be used to describe the structure, only one of these has been highlighted in the diagram for illustrative purposes, marked B (outlined by O1b, N1b, O1d, N1d, O1c, N2b and crowned by N2c). This planar structure is reproduced at each lattice repeat along the a direction so that the atoms of adjacent layers lie directly on top of one another when viewed along this axis. A consequence of this arrangement is that the only bonds between the layers are N1-H \cdots N1 and N2-H \cdots N2 bonds formed between crown ammonia molecules with a length equal to the a lattice parameter.

As can be seen from Figure 6 the crowned chair hexagon arrangement is also found in ice VII. Although the details of the hydrogen bond arrangements differ, the packing of the molecules are remarkably similar to that of ice VII. The left-hand diagram in Figure 6 shows hexagon A crowned by N2b along with a repeat of this unit one unit cell away along the a direction with the N2b'-N2b H-bond providing the bonding between layers. The crowning atom N2b is N-H \cdots O H-bonded to O1a, O1c and O-H \cdots N H-bonded to O1b with H-bond lengths in the range 2.8–3.2 Å. However, this ring is also “crowned” in the other direction by N2b' which has short non-bond contacts to atoms N1b, N2a, and N1a in the range 2.9–3.2 Å to N2b'. The right-hand diagram shows the analogous ring structure in ice VII formed by six oxygen atoms (labelled A to F), this ring is “crowned” on both sides by two oxygen atoms $\kappa 1$ and $\kappa 2$. Although $\kappa 1$ and $\kappa 2$ are not H-bonded to the (A to F) ring they have non-bond $O \cdots O$ contacts which are the same length as the H-bonds to atoms B, D, and F in the case of $\kappa 1$ and atoms A, C, and E in the case of $\kappa 2$ and these contacts are shown as dotted lines. In AHH, the adjacent crowned ring along the a -axis (labelled N1b', etc.) is a lattice repeat away and hence an identical copy, in ice VII it is not and instead $\kappa 2$ forms H-bonds to atoms 2, 4, and 6 of a ring formed of entirely of these short non-bond contacts (again shown as dotted lines). Hexagon B exhibits qualitatively the same geometry as hexagon A with small differences (at the level of 0.1 Å) in the individual interatomic distances and it thus appears that although AHH-II and ice VII have very different H-bond topologies, their molecular packing is rather similar. Given that the molecular packing of ice VII remains stable up to the highest pressures studied,³⁵ it might be expected that AHH-II

(or at least its packing) is also likely to be stable over a large pressure range. The similarities in the molecular packing also suggests that the principal driving force for the formation of this structure is the need to achieve the best possible packing density at the expense of a distortion of the hydrogen bonds. This has also been observed in the high pressure phase IV of ammonia³⁶ and in the case of AHH-II manifests itself in the formation of N-D \cdots N H-bonds. These do not occur in the open ambient pressure structures of the ammonia hydrates, yet in AHH-II they are the only source of bonding between the layers of puckered hexagons.

V. DISCUSSION

It has thus been shown that liquids with a 1:1 ammonia:water molar ratio crystallise to form AHH-II and ice, and we have observed separately that liquids of a 1:2 ammonia:water also form the same phases, as have Fortes *et al.*¹³ This very strongly suggests that the melting point minima at the 1:1 and 1:2 compositions which at ambient pressure result in the formation of the ADH and AMH crystalline structures have disappeared once a pressure of 3.5(1) GPa has been reached. Instead, there is no melting point minimum between pure water and the 2:1 ammonia water composition. Thus, the dehydration boundary reported by Boone and Nicol, and Fortes *et al.* does not just signal the upper pressure limit of the ADH composition in the solid, as they reported, but also the upper limit of the AMH composition. This conclusion also appears to conflict with our earlier work on the molecular alloy AMH-VI which, once formed by compression at low temperature and warming to RT at ~ 5 GPa, remains stable up to at least 10 GPa.¹⁶ This molecular alloy structure is also adopted by ADH when taken along the same thermodynamic path.⁹ It is not clear whether AMH-VI is more stable than AHH-II and ice VII, but since they exist at the same pressures and temperatures, one of them must be metastable. The fact that the AMH-VI structure, AHH-II, and ice VII all have similar molecular packings would suggest that they are close in density and hence in free energy. The fact that solutions crystallise into AHH-II and ice VII strongly suggests that this mixture may be the thermodynamically stable form (at least at 3.5 GPa), but this is not conclusive and further work is needed to settle the question. However, whether or not AHH and ice is thermodynamically stable form, the fact remains that ammonia water solutions reproducibly crystallise into AHH-II and ice VII at room temperature. The presence of a dehydration process all the way to AHH has potential consequences for the behaviour of ammonia inside planetary bodies. The ammonia content of the planetary nebula in the vicinity of Saturn is estimated in the range 10–15% which would correspond to a composition of roughly half ADH and half ice by molar fraction.⁶ Our results suggest that above 3.5(1) GPa in any body where solid phases form, this mixture will be $\sim 80\%$ ice and $\sim 20\%$ AHH. Our measurements show that at this pressure ice VII is 26% denser than AHH-II. This means that above this pressure there this density difference will produce a tendency for the ice to fall towards the centre of the planet whereas the AHH will tend to rise. This differentiation provides a source of heat from the gravitational energy

of the falling material. This causes layering, which will have consequences for convection. This will be important for models of heat flow inside planetary bodies. Finally, the fact that the greater part of any ice layer will be composed of water-ice free from any ammonia content provides an important constraint for the conductivity and other properties. Finally, it is important to note that AHH-II has a wide range of O-D...N, N-D...O, and N-D...N hydrogen bonds of differing lengths and geometry. If, as appears possible, it is stable over a wide pressure range it will provide a good system to explore the effects of changing geometry on H-bond strength over a wide range of densities without the complications of the abrupt structural changes brought about by structural phase transitions.

ACKNOWLEDGMENTS

We would like to thank Richard Nelmes for his advice throughout the work and for his comments on the manuscript, and Malcolm McMahon and Ingo Loa for assistance with the single crystal x-ray studies which were carried out as part of European Synchrotron Radiation Facility (ESRF) long-term proposal hs3090. This work was supported by the U.K. Engineering and Physical Sciences Research Council through grant funding and a studentship for C.W. through the Scottish Doctoral Training Centre in Condensed Matter Physics, and by the Science and Technology Facilities Council through access to beam time and other facilities.

- ¹G. A. Jeffrey, *J. Mol. Struct.* **322**, 21 (1994).
- ²W. W. Cleland and M. M. Kreevoy, *Science* **264**, 1887 (1994).
- ³M. Benoit and D. Marx, *ChemPhysChem* **6**, 1738 (2005).
- ⁴J. S. Loveday and R. J. Nelmes, *High Press. Res.* **24**, 45 (2004).
- ⁵D. R. Allan, S. J. Clark, R. M. Ibberson, S. Parsons, C. R. Pulham, and L. Sawyer, *Chem. Commun. (Cambridge)* **1999**, 751.
- ⁶T. Guillot, *Annu. Rev. Earth Planet Sci.* **33**, 493 (2005).
- ⁷J. I. Lunine and D. J. Stevenson, *Icarus* **70**, 61 (1987).
- ⁸W. B. Hubbard, M. Podolak, and D. J. Stevenson, in *Neptune and Triton*, edited by D. Cruikshank (Arizona University Press, Tucson AZ, 1995), pp. 109–138.
- ⁹J. S. Loveday, R. J. Nelmes, C. L. Bull, H. E. Maynard-Casely, and M. Guthrie, *High Press. Res.* **29**, 396 (2009).
- ¹⁰A. D. Fortes, I. G. Wood, L. Vočadlo, K. S. Knight, W. G. Marshall, M. G. Tucker, and F. Fernandez-Alonso, *J. Appl. Crystallogr.* **42**, 846 (2009).
- ¹¹M. L. Johnson and M. Nicol, *J. Geophys. Res.* **92**, 6339, doi:10.1029/JB092iB07p06339 (1987).
- ¹²S. Boone and M. F. Nicol, *Proceedings of Lunar and Planetary Science Conference* (Lunar and Planetary Science Institute, Houston, TX, 1991), Vol. 21, p. 603.
- ¹³A. D. Fortes, I. G. Wood, M. Alfredsson, L. Vočadlo, K. S. Knight, W. G. Marshall, M. G. Tucker, and F. Fernandez-Alonso, *High Press. Res.* **27**, 201 (2007).
- ¹⁴D. Hogenboom, *Icarus* **128**, 171 (1997).
- ¹⁵J. S. Loveday and R. J. Nelmes, in *Proceedings of the XVIIIth AIRAPT Conference* (University Press, Hyderabad, India, 2000), Vol. 1, p. 133.
- ¹⁶J. S. Loveday and R. J. Nelmes, *Phys. Rev. Lett.* **83**, 4329 (1999).
- ¹⁷A. D. Fortes, E. Suard, C. J. Pickard, and R. J. Needs, *J. Am. Chem. Soc.* **135**, 13508 (2009).
- ¹⁸A. D. Fortes, J. P. Brodholt, I. G. Wood, L. Vočadlo, and H. D. B. Jenkins, *J. Chem. Phys.* **115**, 7006 (2001).
- ¹⁹A. D. Fortes, E. Suard, M.-H. Lemée-Cailleau, C. J. Pickard, and R. J. Needs, *J. Chem. Phys.* **131**, 154503 (2009).
- ²⁰A. D. Fortes, I. G. Wood, J. P. Brodholt, M. Alfredsson, L. Vočadlo, G. S. McGrady, and K. S. Knight, *J. Chem. Phys.* **119**, 10806 (2003).
- ²¹A. D. Fortes, *Icarus* **162**, 59 (2003).
- ²²R. J. Nelmes, J. S. Loveday, and M. Guthrie, *ISIS Annual Report* 1999.
- ²³Deuterated samples were used to avoid the high incoherent background scattering from hydrogen.
- ²⁴L. Merrill and W. A. Bassett, *Rev. Sci. Instrum.* **45**, 290 (1974).
- ²⁵J. M. Besson, R. J. Nelmes, G. Hamel, J. S. Loveday, G. Weill, and S. Hull, *Physica B* **180–181**, 907 (1992).
- ²⁶R. M. Wilson, J. S. Loveday, R. J. Nelmes, S. Klotz, and W. G. Marshall, *Nucl. Instrum. Methods Phys. Res. A* **354**, 145 (1995).
- ²⁷XPREP version 2005/2, Sheldrick, Bruker AXS Inc.
- ²⁸R. J. Hemley, A. P. Jephcoat, H. K. Mao, C. S. Zha, L. W. Finger, and D. E. Cox, *Nature (London)* **330**, 737 (1987).
- ²⁹J. S. Loveday and R. J. Nelmes, *High Press. Res.* **23**, 41 (2003).
- ³⁰V. Favre-Nicolin and R. Černý, *J. Appl. Crystallogr.* **35**, 734 (2002).
- ³¹V. Favre-Nicolin and R. Černý, *Z. Kristallogr.* **219**, 847 (2004).
- ³²The goodness-of-fit combines the quality of fit to the data (χ^2) and the degree to which any user imposed structural constraints are obeyed. In this case, no constraints were used and hence the (G-o-F) is proportional to χ^2 .
- ³³A. C. Larson and R. Dreele, Los Alamos National Laboratory Report, 2004.
- ³⁴The refined parameters were the fractional co-ordinates of all the atoms (33 parameters total), 14 background co-efficients for the two histograms, 6 thermal parameters (2 for AHH, 2 for tungsten carbide (anvil material), and 2 for Ice VII), lattice parameters of all phases in profile (7 total, 4 for AHH-II, 2 for tungsten-carbide, 1 for Ice VII), 8 profile co-efficients (sigma-1 and gamma-1 for all phases in transverse data, and only AHH phase in longitudinal data) scale factors of both longitudinal and transverse data sets and two phase fractions (for ice and tungsten carbide), two diffractometer constants for the longitudinal data and one for the transverse data, and the absorption co-efficient.
- ³⁵P. Loubeyre, R. LeToullec, E. Wolanin, M. Hanfland, and D. Häusermann, *Nature(London)* **397**, 503 (1999).
- ³⁶J. S. Loveday, R. J. Nelmes, W. G. Marshall, J. Besson, S. Klotz, and G. Hamel, *Phys. Rev. Lett.* **76**, 74 (1996).
- ³⁷F. Sohl, *Proceedings of the 263rd International-Astronomical-Union (IAU) Symposium* (Cambridge University Press, Cambridge, UK, 2009), Vol. 5, p. 113.
- ³⁸J. E. Bertie, *J. Chem. Phys.* **78**, 6203 (1983).
- ³⁹J. E. Bertie and J. P. Devlin, *J. Chem. Phys.* **79**, 2092 (1983).
- ⁴⁰J. E. Bertie and J. P. Devlin, *J. Chem. Phys.* **81**, 1559 (1984).
- ⁴¹W. C. Hamilton, *Acta Crystallogr.* **18**, 502 (1965).